*International Journal of Engineering Applied Sciences and Technology, 2022*
**Vol. 7, Issue 4, ISSN No. 2455-2143, Pages 31-44**
Published Online August 2022 in IJEAST (http://www.ijeast.com)

# ACID HYDROLYSIS OF CORN COB TO GLUCOSE: A KINETIC STUDY

O.E. Onyelucheya, B.N. Uzoh, J.C. Obijiaku
[1]Department of Chemical Engineering,
Federal University of Technology, P.M.B 1526, Owerri, Nigeria.

Ralph E. Martin
Department of Chemical Engineering,
University of Arkansas, Fayetteville, AR 72701,USA.

***Abstract:*** **Corn cob is a renewable, cheap and abundant lignocellulosic material. Being a potential source of fermentable sugars, corn cob can be used as a substrate for value added products such as ethanol. This research work studied the glucose production from corn cob using phosphoric and nitric acids at $130^0$C, acid concentrations of 1wt%, 2wt%, 3wt%, 4wt% and 5wt% respectively and at time intervals of 18mins, 36mins,54mins,72mins and 90mins respectively. The substrate was characterized for the proximate constituents and the results show that corn cob has high hemicellulosic content. Seaman model and the Two-fraction model were used in studying the kinetics of glucose concentration in the hydrolysates, and the Two-fraction model gave a better fit with $R^2$ equal to 1. A maximum concentration of 0.038mg/ml of glucose was produced when 5wt% $H_3PO_4$ was used as catalyst for the hydrolysis, and a time interval of 42mins, with 0.4% susceptibility to hydrolysis. Whereas for the nitric acid hydrolysis, 0.054mg/ml maximum concentration of glucose was produced using 2wt% of $HNO_3$, at a time interval of 77mins, with 0.6% susceptibility to hydrolysis. Comparatively, nitric acid proved to be a more efficient catalyst for acid hydrolysis of corn cobs.**

***Key Words:*** **Corn cob, Acid hydrolysis, Glucose, Lignocellulosic material, Seaman's model, Two-fraction model.**

## I. INTRODUCTION

Agricultural residue can be referred to as lignocellulosic material. This is a low cost and the most abundant renewable energy source in the world. Examples of agricultural residues are corn cob, sugar cane bagasse, hardwood, softwood. corn stover, rice stover, wheat straw, and grasses etc. (Yuan et al., 2021).

With this economic advantage attached to lignocellulosic materials, it can be converted to useful products through hydrolysis(Wan et al., 2021). The hydrolysis of corn cobs to produce glucose solutions could be a good alternative use for this abundant resource (Delbecqet al., 2018).

In diversifying the use of global renewable energy through better alternative sources there is need to convert agricultural residue which are in abundance to useful products such as ethanol (Guo et al., 2018). Acid hydrolysis being the method applied, this research work tends to determine between phosphoric and nitric acids which is preferable in the process of converting agricultural residual to useful products. Ethanol can serve as an alternative to transportation fuel, reduce greenhouse gas emission. There is need to properly understand the application of the kinetic models which were used to explain the variation with time of the main products generated and the optimal yield of glucose (Alessandra et al., 2012).

Corn cob is rich in glucose among all other lignocellulosic materials, making it a potential source of value-added products. Therefore, the hydrolysis of corn cob could be a good alternative for glucose production which could further be broken down to ethanol for further end use (Onyelucheyaet al., 2016).

Economic interest in ethanol production can be enhanced if the required glucose solutions can be obtained from the hydrolysis of low-cost lignocellulosic wastes (Kalyaniet al., 2017).

This research paper focuses on the study of the concentration of glucose yield during acid hydrolysis of corn cob at a constant temperature of $130^0$c, for time intervals of 18mins, 36mins, 54mins, 72mins and 90mins and concentrations of 1wt%, 2wt%, 3wt%, 4wt% and 5wt % of both Phosphoric and Nitric acids ($H_3PO_4$ and $HNO_3$) respectively, and to determine the rate constants and other kinetic parameters of the individual acid hydrolysis process and to maximize production for the sugar of interest.

## II. LITERATURE REVIEW AND THEORITICAL BACKGROUND

### 2.1 Kinetic Study of Lignocellulosic Material with Acids

#### 2.1.1 Kinetic Modeling of Lignocellulosic Material

*International Journal of Engineering Applied Sciences and Technology, 2022*
**Vol. 7, Issue 4, ISSN No. 2455-2143, Pages 31-44**
Published Online August 2022 in IJEAST (http://www.ijeast.com)

Saeman and Two fraction models are the two kinetic models mostly proposed to investigate the acid hydrolysis of lignocellulosic materials by different researchers (Onyelucheyaet al., 2016).

**2.1.2 Saeman's Model**

The simplified models for the study of the kinetics of hydrolysis process using acids began with the work of Saeman for the hydrolysis of douglas fire wood using sulphuric acid (Saeman, 1945). In his research the hydrolysis of cellulose was studied establishing the following model:

$$\text{Cellulose} \xrightarrow{K_1} \text{Glucose} \xrightarrow{K_2} \text{Decomposition products}$$

where $k_1(min^{-1})$ is the rate for release of glucose from cellulose and $k_2(min^{-1})$ is rate for glucose decomposition. This model considers the hydrolysis of cellulose to release glucose that in severe conditions is decomposed.

Eken-Saracglu et al. (1998) applied the Seaman's modes in their study done on kinetic comparative of hemicelluloses hydrolysis in corn cob and sun flower seed hull. The model was also applied in the works of Esther et al. (2012), for the hydrolysis of the hemicelluloses fraction of wheat straw using sulphuric acid. Onyelucheyaet al. (2016) in their study on acid hydrolysis of cassava peel applied similar models. Liang et al. (2017) in the effort to study the acid hydrolysis of corncobs to levulinic acid applied the Saeman's models. The models were helpful to da Costa Lopes&Łukasik (2018) in their work on separation and recovery of a hemicellulose-derived sugar produced from the hydrolysis of biomass by an acidic ionic liquid. Also, Wang et al. (2019) adopted the Saeman's models in their kinetic study on the hydrolysis of corncob residues to levulinic acid. And Yuan et al. (2021) equally applied the models in their kinetics studies on the hydrolysis of hemicellulose.

The model of Saeman can therefore be generalized for any polymer as:

$$\text{Polymer} \xrightarrow{K_1} \text{Monomer} \xrightarrow{K_2} \text{decomposition}$$

The generalized polymer could be cellulose, hemicellulose, etc.

where $K_1$ = Rate of generation reaction and $K_2$ = Rate of decomposition reaction, and:

$$r_A = d\frac{C_A}{dt} = -k_1 C_A \quad (2.1)$$

$$r_B = d\frac{C_B}{dt} = -k_1 C_A - K_2 C_B \quad (2.2)$$

$$r_C = d\frac{C_C}{dt} = k_2 C_B \quad (2.3)$$

where $C_A$ = Polymer concentration
$C_B$ = Monomer concentration
$C_C$ = Decomposition product concentration

From equation (2.1)

$$d\frac{C_A}{dt} = -k_1 C_A$$

$$\int_{CA_0}^{C_A} \frac{dC_A}{C_A} = -k_1 \int_0^t dt$$

$$\ln\frac{C_A}{CA_0} = -K_1 t$$

$$C_A = C_{A0} e^{-K_1 t} \quad (2.4)$$

Where; $C_{AO}$ = Initial Polymer concentration

Substituting equation (2.1) into (2.2)

$$\frac{dC_B}{dt} = k_1 C_{A0} e^{-K_1 t} - k_2 C_B$$

$$\frac{dC_B}{dt} + k_2 C_B = k_1 C_{A0} e^{-K_1 t} \quad (2.5)$$

Equation (2.5) can be solved by Laplace transform or integrating factors.

Applying Laplace transform to equation (2.5);

$$L\left[\frac{dC_B}{dt}\right] + k_2 L[C_B] = k_1 C_{A0} L\left[e^{-k_1 t}\right]$$

$$L\left[\frac{dC_B}{dt}\right] = -k_2 L[C_B] + k_1 C_{A0} L\left[e^{-k_1 t}\right]$$

$$s\,C_B(s) - C_B(0) = -k_2 C_B(s) + \frac{k_1 C_{A0}}{S + k_1}$$

$C_B(0) = 0$ Because there is no monomer yet at time 0 sec.

$$sC_B(s) = -k_2 C_B(s) + \frac{k_1 C_{A0}}{S + k_1}$$

$$sC_B(s) + k_2 C_B(s) = \frac{k_1 C_{A0}}{S + k_1}$$

$$C_B(s)[s + k_2] = \frac{k_1 C_{A0}}{[S + k_1]}$$

$$C_B(s) = \frac{k_1 C_{A0}}{(S+k_1)(S+k_2)} \quad (2.6)$$

Resolve equation (2.6) into partial fraction

$$\frac{k_1 C_{A0}}{(S + k_1)(S + k_2)} = \frac{A}{(S + k_1)} + \frac{B}{(S + k_2)}$$

$$k_1 C_{A0} = A(s + k_2) + B(s + k_1)$$

Let s= - $k_1$

$$k_1 C_{A0} = A(k_2 - k_1)$$

$$A = \frac{k_1 C_{A0}}{(k_2 - k_1)} \quad (2.7)$$

Let s = -$k_2$

$$k_1 C_{A0} = A(-k_2 + k_2) + B(k_1 - k_2)$$

$$B = \frac{k_1 C_{A0}}{(k_1 - k_2)} \quad (2.8)$$

$$C_B(s) = \frac{k_1 C_{A0}}{(S+k_1)(S+k_2)} = \frac{k_1 C_{A0}}{(k_2 - k_1)(S+k_1)} + \frac{k_1 C_{A0}}{(k_1 - k_2)(S+k_2)} \quad (2.9)$$

$$C_B(s) = \frac{k_1 C_{A0}}{(k_2 - k_1)(s + k_1)} - \frac{k_1 C_{A0}}{(k_2 - k_1)(s + k_2)}$$

*International Journal of Engineering Applied Sciences and Technology, 2022*
**Vol. 7, Issue 4, ISSN No. 2455-2143, Pages 31-44**
Published Online August 2022 in IJEAST (http://www.ijeast.com)

$$C_B(s) = \frac{k_1 C_{A0}}{(k_2 - k_1)} \left[ \frac{1}{(s+k_1)} - \frac{1}{(s+k_2)} \right] \quad (2.10)$$

Find the Laplace inverse of equation (2.10)

$$C_B(t) = \frac{k_1 C_{A0}}{(k_2 - k_1)} [e^{-k_1 t} - e^{-k_2 t}] \quad (2.11)$$

where; t = time

$C_{A0}$ can be determined analytically by equation (2.12)

$$C_{A0} = \frac{FZ\rho}{WSR} \quad (2.12)$$

Where;

F= stoichiometric factor due to hydration of molecule during the hydrolysis

ρ= density of hydrolysate

z = composition of the raw material for the polysaccharides

WSR = water to solid ratio.

### 2.1.3 Two Fraction Model

Due to the limitation of Saeman's model to only one fraction of the polymer there was need to get an alternative called the Two fraction model which considered a susceptible or fast fraction and a less susceptible or slow fraction, as applied in the work of Aguilar et al. (2002) and da Costa Lopes & Lukasik (2018), where the Two fraction kinetic model showed a better fit as compared to the Saeman's model.

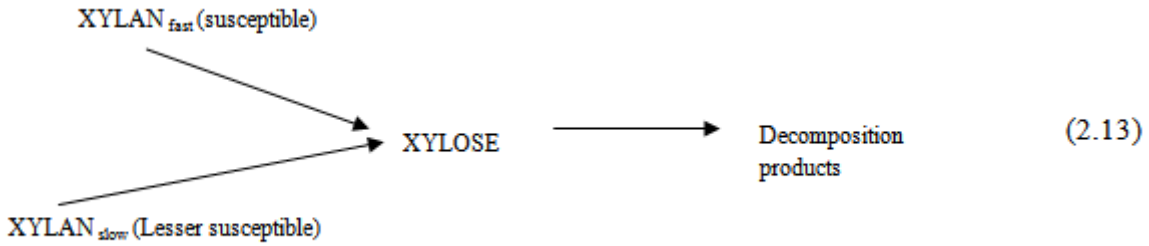


(2.13)

The ratio between the two fractions is the measured for the parameter ∝ which is the mass fraction of the susceptible polymer in the raw material as shown in equation (2.14):

$$\propto = \frac{fast\ xylan}{total\ xylan} \quad (2.14)$$

The lesser susceptible fraction does not react, remaining always in the solid phase. Then the equation that governs the kinetics is;

$$C_B(t) = \frac{\propto k_1 C_{A0}}{(k_2 - k_1)} [e^{-k_1 t} - e^{-k_2 t}] \quad (2.15)$$

## 2.2Comparing the Kinetic Parameters Based on Previous Research

### 2.2.1 Kinetic Modeling of Glucose Concentration

Glucose is the by-product obtained in the acid hydrolysis of lignocellulosic materials. Glucose released can either be from hemicellulose, heteropolymers and cellulose. Glucose from cellulose is not usually hydrolysed in the range of operational condition for acid hydrolysis of hemicellulose (Onyelucheyaet al., 2016; Shi et al., 2017; Yuan et al., 2021).

A review of previous work that used similar substrate but different acids at constant temperature for glucose production is given below:

Aguilar et al. (2002) studied the kinetics for glucose concentration with sulfuric acid and using sugarcane bagasse as a substrate. They applied equation (2.12) to determine $C_{A0}$.

$$C_{A0} = \frac{F\ z\ \rho}{WS\ R} \quad (2.12)$$

$$C_{A0} = \frac{180}{162}\ x\ \frac{38.9}{10}\ x\ 10 = 43.2 g/l$$

They applied the two-fraction model to generate kinetic parameters, $k_1, k_2\ and \propto$ and also the statistical parameter ($R^2$) as shown in Table 2.1.

Table 2.1: Kinetic and statistical parameters of glucose released from the $H_2S0_4$ hydrolysis of sugarcane bagasse (Aguilar et al., 2002)

| **Operational set** | $\propto_G (g/g)$ | $k_1 x\ 10^3 (min^{-1})$ | $k_2 x\ 10^3 (min^{-1})$ | $R^2$ |
|---|---|---|---|---|
| 2% $H_2SO_4$ at 122 $^0$C | 0.121 | 35.7 | 0.29 | 0.979 |
| 4% $H_2SO_4$ at 122 $^0$C | 0.1460 | 84.2 | 0.42 | 0.997 |
| 6% $H_2SO_4$ at 122 $^0$C | 0.182 | 74.1 | 0 | 0.995 |

*International Journal of Engineering Applied Sciences and Technology, 2022*
**Vol. 7, Issue 4, ISSN No. 2455-2143, Pages 31-44**
Published Online August 2022 in IJEAST (http://www.ijeast.com)

$k_1$ = rate of generation reaction from glucan to glucose $(min^{-1})$
$k_2$ = rate of decomposition reaction from glucose to HMF $(min^{-1})$

At $122^0$C, kinetic parameters of glucose generation tends to increase with increase in acid concentration whereas the decomposition reactions of glucose ($k_2$) are negligible.
Sara et al. (2006)studied the hydrolysis of sugarcane bagasse using phosphoric acid. They applied the two-fraction model and generated kinetic parameters as shown in table 2.2.

Table 2.2 Results of fitting the kinetic models(Sara et al., 2006)

| **Operational set** | $\propto_G (g/g)$ | $k_1 x\ 10^3 (min^{-1})$ | $k_2 x\ 10^3 (min^{-1})$ | $R^2$ |
|---|---|---|---|---|
| 2% $H_3PO_4$at 122 $^0$C | 0.09 | 2.38 | 0.000 | 0.99 |
| 4% $H_3PO_4$at 122 $^0$C | 0.08 | 3.84 | 0.003 | 0.99 |
| 6% $H_3PO_4$at 122 $^0$C | 0.08 | 4.90 | 0.305 | 0.99 |

From the table, their result followed similar trend with the work of Aguilar et al., (2002) which showed that the values of $k_1$increased with the phosphoric acid concentration whereas the decomposition reactions of glucose ($k_2$) are negligible.

Antonio et al. (2004), in their work on kinetic assessment of sugarcane bagasse applied Saeman's model and Two-fraction model, Two fraction models gave a better fit than the Seaman's model as shown in Table 2.3.

Table 2.3: Results of the fitting for glucose concentration in the hydrolysis of sugar cane bagasse with nitric acid.(Antonio et al., 2004)

| **Operational set** | **Saeman's model** | | | **Two-fraction model** | | | |
|---|---|---|---|---|---|---|---|
| | $k_2 x\ 10^3$ | $k_1 (min^{-1})$ | $r^2$ | $\propto_G (g/g)$ | $k_1 (min^{-1})$ | $k_2 x\ 10^3 (min^{-1})$ | $r^2$ |
| 2% $HN0_3$ *at* $100^0C$ | 16.4 | 7.6 | 0.993 | 0.04 | 0.021 | 0.0 | 0.996 |
| 4% $HN0_3$ *at* $100^0C$ | 15.8 | 1.2 | 0.899 | 0.06 | 0.026 | 0.0 | 0.942 |
| 6% $HN0_3$ *at* $100^0C$ | 17.7 | 1.6 | 0.943 | 0.07 | 0.031 | 0.0 | 0.984 |
| 2% $HN0_3$ *at* $122^0C$ | 0.4 | 0.3 | 0.990 | 0.53 | 0.001 | 0.0 | 0.990 |
| 4% $HN0_3$ *at* $122^0C$ | 3.6 | 1.4 | 0.859 | 0.16 | 0.011 | 0.0 | 0.871 |
| 6% $HN0_3$ *at* $122^0C$ | 22.9 | 3.8 | 0.801 | 0.10 | 0.127 | 0.3 | 0.997 |
| 2% $HN0_3$ *at* $128^0C$ | 12.7 | 0.9 | 0.811 | 0.21 | 0.004 | 6.3 | 0.888 |
| 4% $HN0_3$ *at* $128^0C$ | 14.9 | 2.0 | 0.761 | 0.09 | 0.042 | 0.1 | 0.999 |
| 6% $HN0_3$ *at* $128^0C$ | 12.6 | 2.0 | 0.780 | 0.10 | 0.034 | 0.0 | 0.976 |

The first three sets are at operating conditions of temperature of $100^o$Cand acid concentration at 2wt%, 4wt% and 6wt% $HN0_3$ respectively. The next three sets are at operating conditions of $122^o$Cand acid concentration at 2wt%, 4wt% and 6wt% $HN0_3$ respectively. The last three sets are at operating condition of $128^o$Cand at 2wt, 4wt and 6wt% $HN0_3$ respectively. They had similar conclusion with that of Aguilar et al. (2002), they concluded that $k_1$ increased with nitric acid concentration but the decomposition of glucose was negligible, being the coefficient affected either by temperature or nitric acid concentration.

## III. MATERIALS AND METHOD

### 3.1 Material acquisition

The corn cobs used for the experiments were gathered from local farmers in Obodoukwu Community in Idea to North LGA of Imo State, Nigeria. The fresh corn cobs (as shown in Fig 3.1) were gathered, sun dried for about three days, to effectively reduce the moisture content and surface wetness of the raw sample.

Figure 3.1: Fresh corn cobs undergoing sun drying

### 3.2 Pretreatment of Fresh Corn Cobs

After the fresh corn cobs has been sun-dried, they were taken to the grinding machine for particle size reduction to

*International Journal of Engineering Applied Sciences and Technology, 2022*
**Vol. 7, Issue 4, ISSN No. 2455-2143, Pages 31-44**
Published Online August 2022 in IJEAST (http://www.ijeast.com)

powdered form. The ground corn cobs (hydrolysis substrate) were then taken to laboratory, screened through a 1.0 mm mesh size, as shown in Fig 3.2, and stored in a container in a cool dry place, from where samples were taken and analyzed to determine some proximate parameters cellulose, hemicellulose, lignin, ash, carbohydrate and the moisture content.

Figure 3.2: Screened Corn Cobs

**3.3 Acid Hydrolysis of the Corn Cobs**

20g of the sample (substrate) was weighed into a 500ml conical flask (reaction vessel). 400ml of phosphoric acid solution ($H_3PO_4$) was then added and the mixture swirled carefully, placed on an electro-thermal magnetic stirrer, set at 150rpm and at a temperature of $130^0$C and at the pre chosen time. At the end of the reaction time, the reaction mixture was quenched in a very cold ice-bath. After 2minutes, the content of the conical flask was filtered and labeled appropriately (with regards to reaction time conditions) and kept in a safe place for the glucose tests. The filtrate samples were afterwards taken to the uv-spectrophotometer for the absorbance readings, at a wavelength of 540nm. For the filtrate sample preparations, DNS reagent was used as outlined in thestandard analytical procedures

The same procedure was used for the nitric acid ($HNO_3$) hydrolysis and reducing sugar test preparations, at different operating time conditions of 18, 36, 54, 72 and 90minutes respectively at a temperatures of $130^0$C, using five different acid concentrations of 1%w/w, 2%w/w, 3%w/w, 4%w/w and 5%w/w respectively.

**3.4 Calibration of Absorbance Reading**

0.2g of glucose was weighed and 100ml of distilled water was added to it to get a stock solution concentration of 20mg/dl. 0.1ml, 0.2ml, 0.3ml, 0.4ml, 0.5ml and 0.6ml were taken with the aid of pipette into six test tubes. A test tube containing blank solution was also prepared. 0.9ml, 0.8ml, 0.7ml, 0.6ml, 0.5ml, and 0.4ml of distilled water were added to each test tube. Also 3ml of DNS reagent was added to each test tube and it was covered with aluminum foil, and the test tubes taken to the hot water bath and heated for 5minutes. Afterwards, 1ml of sodium potassium tartrate was added to each test tube and taken to spectrophotometer set at 540nm wavelength to determine the absorbance reading of glucose at the different concentrations.

All experiments were carried out in duplicates and their average values were used to obtain the concentration values, from the glucose standard calibration curves.

**3.5 Procedure for Absorbance Readings**

The spectrophotometer was switched on and allowed to boot for 30mins before use. The equipment was set to the measuring wavelength (for the sample) of the transmitting light and at 100% transmittance. The cuvettes where cleaned and filled to 4ml of the blank solution, and was inserted into the equipment to calibrate the machine at the set wavelength for that sample, with the blank solution. The blank solution was removed and in turn the cuvette was filled with the sample solutions and insert into the machine to obtain the absorbance readings for the sample solutions, at the set wavelength.

**3.6 Procedure for Obtaining the Kinetic and Statistical Parameters**

The experimental results were converted from absorbance (nm) to concentrations with the aid of the calibration data given.

The concentration values were plotted against time (in minutes). The experimental data were fit to both kinetic models (Saeman & Two fraction) for phosphoric acid and nitric acid with a curve fitting tool in MatLab software, to obtain kinetic parameters ( $k_1 and k_2$ ), $\propto$ and statistical parameter ($Adjusted\ R^2$). where $k_1$ is the rate of monomer generation reaction, $k_2$ is the rate of monomer decomposition reaction while $\propto$ is the mass ratio of susceptible polymer fraction to total polymer (kg kg_1).

## IV. RESULTS AND DISCUSSION

**4.1 Results presentation**

The composition of the corn cob used in this study is shown in Table 4.1. The main fractions of corn cob were in the same range as other herbaceous materials, such as rice, wheat straw and sorghum straw.

To obtain relationship between absorbance and concentration with the aid of curve fitting tool in excel, the absorbance (nm) values were plotted against concentration (mg/dl) values shown in Table 4.2 to obtain the standard calibration curve.

*International Journal of Engineering Applied Sciences and Technology, 2022*
**Vol. 7, Issue 4, ISSN No. 2455-2143, Pages 31-44**
Published Online August 2022 in IJEAST (http://www.ijeast.com)

| Components | Mass fraction (%) |
|---|---|
| Hemicellulose | 42.36 |
| Cellulose | 31.26 |
| Lignin | 12.25 |
| Ash | 1.85 |
| Carbohydrate | 2.86 |
| Moisture content | 3.35 |
| Others | 6.07 |

Table 4.1: Main component of corn cob used in this study

| Absorbance (nm) | Concentration (mg/dl) |
|---|---|
| 0 | 0.0000 |
| 0.2 | 0.1460 |
| 0.4 | 0.3255 |
| 0.6 | 0.4060 |
| 0.8 | 0.4505 |
| 1.0 | 0.4695 |

Table 4.2: Calibration data for glucose (540nm)

**4.1.1 Experimental Result for Glucose Using Phosphoric Acid**

The experimental results of glucose concentration after conversion of its absorbance reading for phosphoric acids are given in Tables 4.3, 4.4, 4.5, 4.6, and 4.7.

| Time (min) | $G_1$ (nm) | $G_2$(nm) | $G_{average}$ (nm) | G (mg/ml) |
|---|---|---|---|---|
| 0 | 0 | 0 | 0 | 0 |
| 18 | 0.926 | 0.908 | 0.917 | 0.0327 |
| 36 | 1.023 | 1.087 | 1.055 | 0.0376 |
| 54 | 0.945 | 1.049 | 0.997 | 0.0356 |
| 72 | 0.812 | 0.818 | 0.815 | 0.0291 |
| 90 | 0.777 | 0.773 | 0.775 | 0.0277 |

Table 4.3: Experimental result for the glucose released at 1wt% phosphoric acid

| Time (min) | $G_1$ (nm) | $G_2$(nm) | $G_{average}$ (nm) | G (mg/ml) |
|---|---|---|---|---|
| 0 | 0 | 0 | 0 | 0 |
| 18 | 0.914 | 0.910 | 0.912 | 0.0325 |
| 36 | 1.156 | 0.986 | 1.071 | 0.0382 |
| 54 | 0.979 | 0.983 | 0.981 | 0.0351 |
| 72 | 0.840 | 0.862 | 0.851 | 0.0304 |
| 90 | 0.912 | 0.838 | 0.875 | 0.0312 |

Table 4.4: Experimental result for the glucosereleased at 2wt% phosphoric acid

| Time (min) | $G_1$ (nm) | $G_2$(nm) | $G_{average}$ (nm) | G (mg/ml) |
|---|---|---|---|---|
| 0 | 0 | 0 | 0 | 0 |
| 18 | 0.842 | 0.864 | 0.853 | 0.0305 |
| 36 | 1.125 | 0.917 | 1.021 | 0.0364 |
| 54 | 0.995 | 1.025 | 1.010 | 0.0361 |
| 72 | 0.936 | 0.904 | 0.920 | 0.0329 |
| 90 | 0.805 | 0.813 | 0.809 | 0.0289 |

Table 4.5: Experimental result for the glucose released at 3wt% phosphoric acid

| Time (min) | $G_1$ (nm) | $G_2$(nm) | $G_{average}$ (nm) | G (mg/ml) |
|---|---|---|---|---|
| 0 | 0 | 0 | 0 | 0 |
| 18 | 0.873 | 0.865 | 0.873 | 0.0312 |
| 36 | 1.036 | 1.038 | 1.037 | 0.0371 |
| 54 | 0.978 | 0.965 | 0.969 | 0.0346 |
| 72 | 0.839 | 0.843 | 0.841 | 0.0305 |
| 90 | 0.709 | 0.693 | 0.701 | 0.0254 |

Table 4.6: Experimental result for the glucose released at 4wt% phosphoric acid

| Time (min) | $G_1$ (nm) | $G_2$(nm) | $G_{average}$ (nm) | G (mg/ml) |
|---|---|---|---|---|
| 0 | 0 | 0 | 0 | 0 |
| 18 | 0.859 | 0.865 | 0.862 | 0.0308 |
| 36 | 1.040 | 1.042 | 1.041 | 0.0371 |
| 54 | 1.014 | 1.010 | 1.012 | 0.0362 |
| 72 | 0.957 | 0.965 | 0.961 | 0.0344 |
| 90 | 0.803 | 0.789 | 0.796 | 0.0285 |

Table 4.7: Experimental result for the glucose released at 5wt% phosphoric acid

*International Journal of Engineering Applied Sciences and Technology, 2022*
**Vol. 7, Issue 4, ISSN No. 2455-2143, Pages 31-44**
Published Online August 2022 in IJEAST (http://www.ijeast.com)

Where;
$G_1$ = First absorbance reading
$G_2$ = Second absorbance reading
$G$ = Concentration of glucose in mg/ml
The Kinetic and statistical parameter of glucose released, applying both Seaman's model and Two-fraction model using phosphoric acid are shown in tables 4.8 & 4.9 below.

| Conc (wt%) | $K_1$ $(min^{-1})$ | $K_2$ $(min^{-1})$ | $Adj\ R^2$ |
|---|---|---|---|
| 1 | 0.003451 | 1.257 | 0.8329 |
| 2 | 0.001575 | 0.6082 | 0.9552 |
| 3 | 0.0003283 | 0.1346 | 0.7540 |
| 4 | 0.003137 | 1.177 | 0.9312 |
| 5 | 0.0003196 | 0.1292 | 0.8441 |

Table 4.8: Kinetic and statistical parameter of glucose released for Seaman's model using phosphoric acid

| Conc (wt%) | $K_1$ $(min^{-1})$ | $K_2$ $(min^{-1})$ | $\propto$ | $Adj\ R^2$ |
|---|---|---|---|---|
| 1 | 0.9035 | 0.003451 | 0.02741 | 0.9105 |
| 2 | 0.7644 | 0.002803 | 0.02684 | 0.925 |
| 3 | 0.08389 | 0.005148 | 0.03169 | 0.982 |
| 4 | 0.05453 | 0.01124 | 0.04002 | 0.9758 |
| 5 | 0.05057 | 0.008932 | 0.03917 | 0.9964 |

Table 4.9: Kinetic and statistical parameter of glucose released for Two fraction model using phosphoric acid

To compare the experimental values with values obtained applying the Saeman's model and Two-fraction model at varying concentrations of phosphoric acid for glucose released is shown below.

| Time (min) | Experimental Data (mg/ml) | Saeman's Model (mg/ml) | Two-fraction model (mg/ml) |
|---|---|---|---|
| 0 | 0 | 0 | 0 |
| 18 | 0.0327 | 0.02608 | 0.03606 |
| 36 | 0.0376 | 0.03390 | 0.03789 |
| 54 | 0.0356 | 0.03186 | 0.03484 |
| 72 | 0.0291 | 0.02654 | 0.02993 |
| 90 | 0.0277 | 0.02614 | 0.02812 |

Table 4.10: Comparison of the experimental data with the model at 1wt% phosphoric acid for the glucose released

| Time (min) | Experimental Data (mg/ml) | Saeman's Model (mg/ml) | Two-fraction model (mg/ml) |
|---|---|---|---|
| 0 | 0 | 0 | 0 |
| 18 | 0.0325 | 0.03119 | 0.03572 |
| 36 | 0.0382 | 0.02921 | 0.03896 |
| 54 | 0.0351 | 0.03225 | 0.03429 |
| 72 | 0.0304 | 0.02232 | 0.03069 |
| 90 | 0.0312 | 0.02142 | 0.02919 |

Table 4.11: Comparison of the experimental data withthe model at 2wt% phosphoric acid for the glucose released

| Time (min) | Experimental Data (mg/ml) | Saeman's Model (mg/ml) | Two-fraction model (mg/ml) |
|---|---|---|---|
| 0 | 0 | 0 | 0 |
| 18 | 0.0305 | 0.02487 | 0.03051 |
| 36 | 0.0364 | 0.03342 | 0.03682 |
| 54 | 0.0361 | 0.03347 | 0.03514 |
| 72 | 0.0329 | 0.02629 | 0.03268 |
| 90 | 0.0289 | 0.0231 | 0.02959 |

Table 4.12: Comparison of the experimental data with the model at 3wt% phosphoric acid for the glucose released

| Time (min) | Experimental Data (mg/ml) | Saeman's Model (mg/ml) | Two-fraction model (mg/ml) |
|---|---|---|---|
| 0 | 0 | 0 | 0 |
| 18 | 0.0312 | 0.03522 | 0.03108 |
| 36 | 0.0371 | 0.03328 | 0.03703 |
| 54 | 0.0346 | 0.03146 | 0.03461 |
| 72 | 0.0305 | 0.02973 | 0.02991 |
| 90 | 0.0254 | 0.02809 | 0.02504 |

Table 4.13: Comparison of the experimental data withthe model at 4wt% phosphoric acid for the glucose released

*International Journal of Engineering Applied Sciences and Technology, 2022*
**Vol. 7, Issue 4, ISSN No. 2455-2143, Pages 31-44**
Published Online August 2022 in IJEAST (http://www.ijeast.com)

| Time (min) | Experimental Data (mg/ml) | Saeman's Model (mg/ml) | Two-fraction model (mg/ml) |
|---|---|---|---|
| 0 | 0 | 0 | 0 |
| 18 | 0.0308 | 0.031 | 0.02979 |
| 36 | 0.0371 | 0.03385 | 0.03735 |
| 54 | 0.0362 | 0.03395 | 0.03663 |
| 72 | 0.0344 | 0.03379 | 0.03313 |
| 90 | 0.0285 | 0.03359 | 0.02899 |

Table 4.14: Comparison of the experimental data with the model at 5wt% phosphoric acid for the glucose released

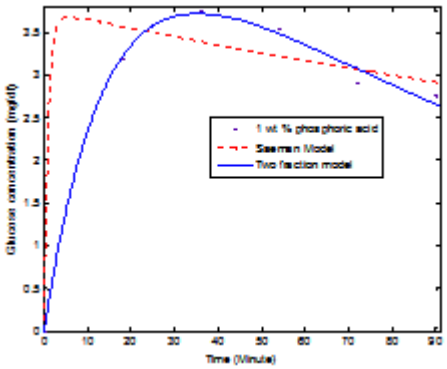


Figure 4.1: The graph for glucose released at 1wt% phosphoric acid

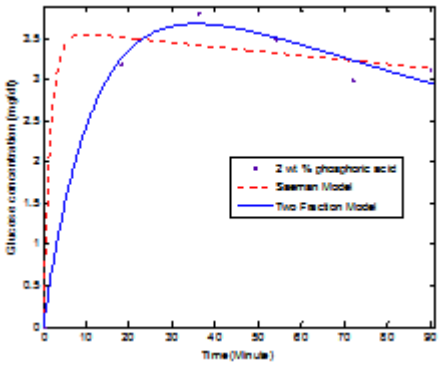


Figure 4.2: The graph for glucose released at 2wt% phosphoric acid

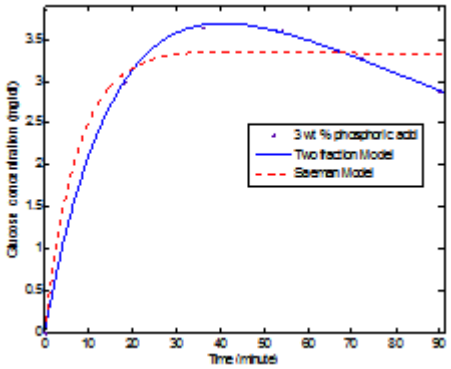


Figure 4.3: The graph for glucose released at 3wt% phosphoric acid

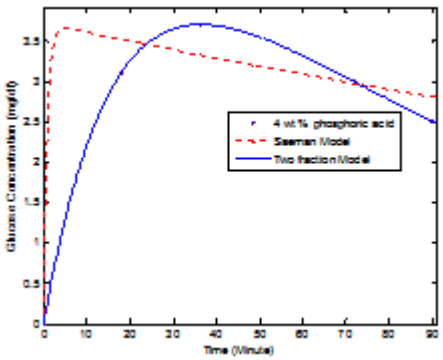


Figure 4.4: The graph for glucose released at 4wt% phosphoric acid

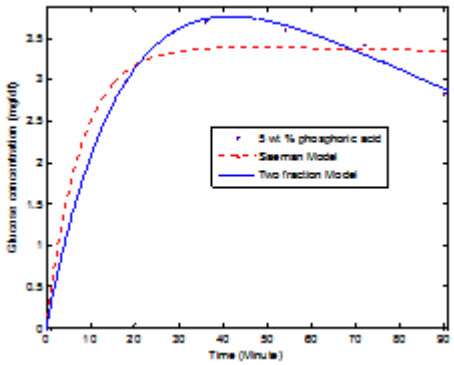


Figure 4.5: The graph for glucose released at 5wt% phosphoric acid

**4.1.2 Experimental Result for Glucose Using Nitric Acid**

The experimental results of glucose concentration after conversion of its absorbance reading for nitric acids are given in Tables 4.15, 4.16 4.17, 4.18, and 4.19.

*International Journal of Engineering Applied Sciences and Technology, 2022*
**Vol. 7, Issue 4, ISSN No. 2455-2143, Pages 31-44**
Published Online August 2022 in IJEAST (http://www.ijeast.com)

| Time (min) | $G_1$ (nm) | $G_2$(nm) | $G_{average}$ (nm) | G (mg/ml) |
|---|---|---|---|---|
| 0 | 0 | 0 | 0 | 0 |
| 18 | 0.760 | 0.744 | 0.752 | 0.0268 |
| 36 | 1.216 | 1.015 | 1.116 | 0.0398 |
| 54 | 1.541 | 1.532 | 1.535 | 0.0548 |
| 72 | 1.546 | 1.546 | 1.546 | 0.0552 |
| 90 | 1.408 | 1.404 | 1.406 | 0.0502 |

Table 4.15: Experimental result for the glucose released at 1wt% nitric acid

| Time (min) | $G_1$ (nm) | $G_2$(nm) | $G_{average}$ (nm) | G (mg/ml) |
|---|---|---|---|---|
| 0 | 0 | 0 | 0 | 0 |
| 18 | 0.562 | 0.556 | 0.559 | 0.0199 |
| 36 | 1.295 | 1.275 | 1.285 | 0.0459 |
| 54 | 1.542 | 1.542 | 1.542 | 0.055 |
| 72 | 1.482 | 1.490 | 1.486 | 0.053 |
| 90 | 1.422 | 1.434 | 1.428 | 0.0509 |

Table 4.16: Experimental result for the glucose released at 2wt% nitric acid

| Time (min) | $G_1$ (nm) | $G_2$(nm) | $G_{average}$ (nm) | G (mg/ml) |
|---|---|---|---|---|
| 0 | 0 | 0 | 0 | 0 |
| 18 | 0.363 | 0.355 | 0.359 | 0.0128 |
| 36 | 0.427 | 0.423 | 0.425 | 0.0152 |
| 54 | 0.420 | 0.425 | 0.4225 | 0.0151 |
| 72 | 0.424 | 0.426 | 0.425 | 0.0152 |
| 90 | 0.424 | 0.426 | 0.425 | 0.0152 |

Table 4.17: Experimental result for the glucose released at 3wt% nitric acid

| Time (min) | $G_1$ (nm) | $G_2$(nm) | $G_{average}$ (nm) | G (mg/ml) |
|---|---|---|---|---|
| 0 | 0 | 0 | 0 | 0 |
| 18 | 0.395 | 0.395 | 0.395 | 0.0141 |
| 36 | 0.426 | 0.425 | 0.426 | 0.0352 |
| 54 | 0.422 | 0.428 | 0.425 | 0.0452 |
| 72 | 1.349 | 1.352 | 1.351 | 0.0482 |
| 90 | 1.347 | 1.350 | 1.349 | 0.0441 |

Table 4.18: Experimental result for the glucose released at 4wt% nitric acid

| Time (min) | $G_1$ (nm) | $G_2$(nm) | $G_{average}$ (nm) | G (mg/ml) |
|---|---|---|---|---|
| 0 | 0 | 0 | 0 | 0 |
| 18 | 0.932 | 0.712 | 0.822 | 0.0293 |
| 36 | 1.343 | 1.343 | 1.343 | 0.0479 |
| 54 | 1.345 | 1.351 | 1.348 | 0.0481 |
| 72 | 1.350 | 1.351 | 1.3505 | 0.0482 |
| 90 | 1.352 | 1.353 | 1.3525 | 0.0483 |

Table 4.19: Experimental result for the glucose released at 5wt% nitric acid

Where;
$G_1$ = First absorbance reading
$G_2$ = Second absorbance reading
$G$ = Concentration of glucose in mg/ml
The Kinetic and statistical parameter of glucose released, applying both Seaman's model and Two-fraction model using nitric acid are shown in tables 4.20 & 4.21 below.

| Conc (wt%) | $K_1$ $(min^{-1})$ | $K_2$ $(min^{-1})$ | $Adj\,R^2$ |
|---|---|---|---|
| 1 | 9.446e-005 | 0.03808 | 0.866 |
| 2 | 8.955e-005 | 0.03534 | 0.8386 |
| 3 | 6.878e-005 | 0.1031 | 0.7993 |
| 4 | 6.545e-005 | 0.02772 | 0.8176 |
| 5 | 0.0001252 | 0.05708 | 0.9813 |

Table 4.20: Kinetic and statistical parameter of glucose released for Seaman's model using nitric acid

| Conc (wt%) | $K_1$ $(min^{-1})$ | $K_2$ $(min^{-1})$ | $\propto$ | $Adj\,R^2$ |
|---|---|---|---|---|
| 1 | 0.01326 | 0.01325 | 0.06351 | 0.9744 |
| 2 | 0.01301 | 0.01302 | 0.06379 | 0.9455 |
| 3 | 0.09755 | 0.0004257 | 0.06817 | 0.9993 |
| 4 | 0.01112 | 0.01114 | 0.0569 | 0.9126 |
| 5 | 0.03497 | 0.005508 | 0.03072 | 0.985 |

Table 4.21: Kinetic and statistical parameter of glucose released for Two fraction model using nitric acid

To compare the experimental values with values obtained applying the Saeman's model and Two-fraction model at varying concentrations of nitric acid for glucose released is show below.

*International Journal of Engineering Applied Sciences and Technology, 2022*
**Vol. 7, Issue 4, ISSN No. 2455-2143, Pages 31-44**
Published Online August 2022 in IJEAST (http://www.ijeast.com)

| Time (min) | Experimental Data (mg/ml) | Saeman's Model (mg/ml) | Two-fraction model (mg/ml) |
|---|---|---|---|
| 0 | 0 | 0 | 0 |
| 18 | 0.0268 | 0.02818 | 0.02736 |
| 36 | 0.0398 | 0.04234 | 0.03911 |
| 54 | 0.0548 | 0.04941 | 0.05394 |
| 72 | 0.0552 | 0.05293 | 0.05551 |
| 90 | 0.0502 | 0.05465 | 0.05269 |

Table 4.22: Comparison of the experimental data with the model at 1wt% nitric acid for the glucose released

| Time (min) | Experimental Data (mg/ml) | Saeman's Model (mg/ml) | Two-fraction model (mg/ml) |
|---|---|---|---|
| 0 | 0 | 0 | 0 |
| 18 | 0.0199 | 0.0273 | 0.02038 |
| 36 | 0.0459 | 0.04172 | 0.04285 |
| 54 | 0.055 | 0.0493 | 0.05086 |
| 72 | 0.053 | 0.05327 | 0.05365 |
| 90 | 0.0509 | 0.05533 | 0.05305 |

Table 4.23: Comparison of the experimental data with the model at 2wt% nitric acid for the glucose released

| Time (min) | Experimental Data (mg/ml) | Saeman's Model (mg/ml) | Two-fraction model (mg/ml) |
|---|---|---|---|
| 0 | 0 | 0 | 0 |
| 18 | 0.0128 | 0.01289 | 0.01286 |
| 36 | 0.0152 | 0.01429 | 0.01498 |
| 54 | 0.0151 | 0.01518 | 0.01525 |
| 72 | 0.0152 | 0.01521 | 0.01520 |
| 90 | 0.0152 | 0.01520 | 0.01509 |

Table 4.24: Comparison of the experimental data with the model at 3wt% nitric acid for the glucose released

| Time (min) | Experimental Data (mg/ml) | Saeman's Model (mg/ml) | Two-fraction model (mg/ml) |
|---|---|---|---|
| 0 | 0 | 0 | 0 |
| 18 | 0.0141 | 0.02124 | 0.02136 |
| 36 | 0.0352 | 0.03412 | 0.03497 |
| 54 | 0.0452 | 0.04191 | 0.04293 |
| 72 | 0.0482 | 0.04661 | 0.04785 |
| 90 | 0.0441 | 0.04944 | 0.04393 |

Table 4.25: Comparison of the experimental data with the model at 4wt% nitric acid for the glucose released

| Time (min) | Experimental Data (mg/ml) | Saeman's Model (mg/ml) | Two-fraction model (mg/ml) |
|---|---|---|---|
| 0 | 0 | 0 | 0 |
| 18 | 0.0293 | 0.02223 | 0.03015 |
| 36 | 0.0479 | 0.04369 | 0.0468 |
| 54 | 0.0481 | 0.04773 | 0.04942 |
| 72 | 0.0482 | 0.04509 | 0.04947 |
| 90 | 0.0483 | 0.04352 | 0.04731 |

Table 4.26: Comparison of the experimental data with the model at 5wt% nitric acid for the glucose released

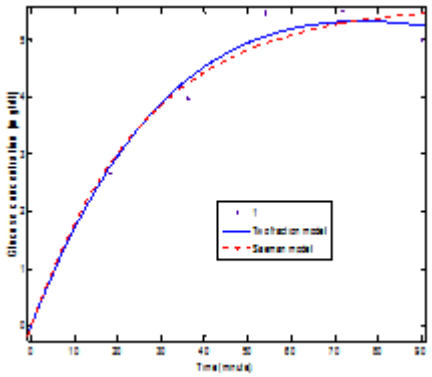

Figure 4.6: The graph for glucose released at 1wt% nitric acid

*International Journal of Engineering Applied Sciences and Technology, 2022*
**Vol. 7, Issue 4, ISSN No. 2455-2143, Pages 31-44**
Published Online August 2022 in IJEAST (http://www.ijeast.com)

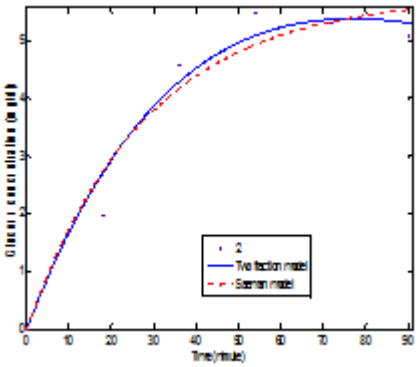


Figure 4.7: The graph for glucose released at 2wt% nitric acid

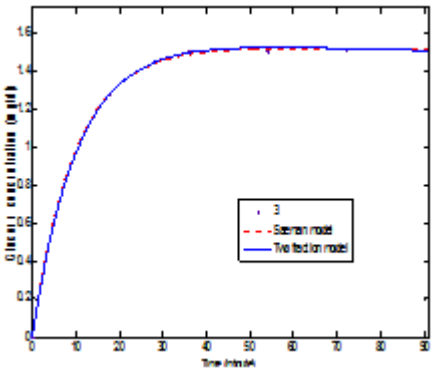


Figure 4.8: The graph for glucose released at 3wt% nitric acid

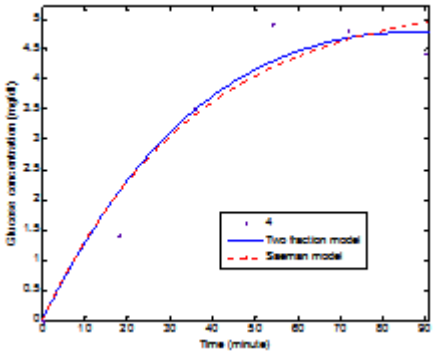


Figure 4.9: The graph for glucose released at 4wt% nitric acid

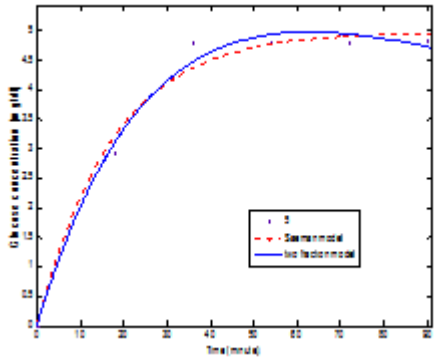


Figure 4.10: The graph for glucose released at 5wt% nitric acid

### 4.2 Discussion of Results

Table 4.1 show the result of proximate analysis of the corn cob used in this study, this analysis shows that it is richer in hemicellulose than cellulose.

The experimental result of glucose concentration for phosphoric acid are given in Tables 4.3, 4.4, 4.5, 4.6, 4.7 and that for nitric acid are given in Tables 4.15, 4.16, 4.17, 4.18, and 4.19 respectively. They were converted from absorbance (nm) to concentration (mg/dl) with the aid of calibration data given in Table 4.2.Also the experimental data were fit to Saeman's model and Two-fraction model.

The data of Table 4.2 was used to obtain the standard calibration curve used for the conversion of the absorbance data (nm) to concentration data (mg/ml), with the help of equation 4.1 showing the relationship between the two variables.

$$\text{Concentration} = \left[\frac{Absorbance}{0.5604}\right] \times 2 \qquad (4.1)$$

Equation (4.1) was used to convert absorbance reading in column four of Table 4.3, 4.4, 4.5, 4.6 and 4.7 for phosphoric acid and Tables 4.15, 4.16, 4.17, 4.18, and 4.19 for nitric acid respectively to concentration in column five of the same tables.

Equation 4.2 is the general Saeman's model equation whereas equations 4.3 and 4.4 are Saeman model used for phosphoric and nitric acids hydrolysis respectively, to yield glucose.

$$C_B(t) = \frac{CAo\,K_1}{(k_2 - k_1)}\left[e^{-k_1 t} - e^{-k_2 t}\right] \qquad (4.2)$$

$$G(t) = \frac{10.5669 K_1}{(K_2 - k_1)}\left[e^{-k_1 t} - e^{-k_2 t}\right] \quad (H_3PO_4) \qquad (4.3)$$

$$G(t) = \frac{14.0644 K_1}{(k_2 - k_1)}\left[e^{-k_1 t} - e^{-k_2 t}\right] \quad (HNO_3) \qquad (4.4)$$

Glucose concentrations $(mg/ml)$ were plotted from Table 4.3, 4.4, 4.5,4.6 and 4.7 for phosphoric acid and Tables 4.15, 4.16, 4.17, 4.18 and 4.19 for nitric acid respectively against time (min), the experimental data were fit to

*International Journal of Engineering Applied Sciences and Technology, 2022*
**Vol. 7, Issue 4, ISSN No. 2455-2143, Pages 31-44**
Published Online August 2022 in IJEAST (http://www.ijeast.com)

equation (4.3) for phosphoric acid and equation (4.4) for nitric acid with curve fitting tool in MatLab software to obtain kinetic parameters ( $k_1 and k_2$ ) and statistical parameter ($Adjusted\ R^2$) as shown in Tables 4.8 and 4.20. The figures for the plots are shown in Figures 4.1, 4.2, 4.3, 4.4 ,4.5, 4.6, 4.7, 4.8, 4.9 and 4.10, for both phosphoric and nitric acids respectively. The values of $k_1$ and $k_2$ were substituted into equation 4.3 and 4.4 to generate Seaman's model data at different concentrations of phosphoric and nitric acids, given in column three of Tables 4.10, 4.11, 4.12, 4.13 and 4.14 for phosphoric acid and Tables 4.22, 4.23, 4.24, 4.25 and 4.26 for nitric acid, respectively.

Equation 4.4 is the general Two-fraction model equation whereas equations 4.6 and 4.7 are Two-fraction model used for phosphoric and nitric acids hydrolysis respectively, to yield glucose.

$$C_B(t) = \frac{CAo\ \alpha K_1}{(k_2 - k_1)}\left[e^{-k_1 t} - e^{-k_2 t}\right] \quad (4.5)$$

$$G(t) = \frac{10.5669 \alpha K_1}{(k_2 - k_1)}\left[e^{-k_1 t} - e^{-k_2 t}\right] \quad (H_3PO_4) \quad (4.6)$$

$$G(t) = \frac{14.0644 \alpha K_1}{(k_2 - k_1)}\left[e^{-k_1 t} - e^{-k_2 t}\right] \quad (HNO_3) \quad (4.7)$$

Glucose concentrations $(mg/ml)$ were plotted from Table 4.3, 4.4, 4.5,4.6 and 4.7 for phosphoric acid and Tables 4.15, 4.16, 4.17,
4.18, and 4.19 for nitric acid respectively against time (min), the experimental data were fit to equation (4.6) for phosphoric acid and equation (4.7) for nitric acid with curve fitting tool in MatLab to obtain kinetic parameters ( $k_1$ and $k_2$ ), $\propto$ and statistical parameter( Adjusted $R^2$), as shown in Table 4.9 and 4.21. The figures for the plots are shown in Figures 4.1, 4.2, 4.3, 4.4, 4.5 ,4.6, 4.7, 4.8, 4.9 and 4.10, for both phosphoric and nitric acids respectively. The values of $k_1$, $k_2$ and $\propto$ were substituted into equation 4.6 and 4.7 to generate Two-fraction model data at different concentrations of phosphoric acid and nitric acids, given in column four of Tables 4.10, 4.11, 4.12, 4.13 and 4.14 for phosphoric acid and Tables 4.22, 4.23, 4.24, 4.25 and 4.26 for nitric acid, respectively.

The glucose concentrations were also fitted into both the Saeman and Two-fraction models for the phosphoric acid hydrolysis as shown in Tables 4.8 and 4.9. Comparing the values of the statistical parameter ( Adjusted $R^2$), it was found that the Two-fraction model fits better. This result agrees with those of Aguilar et al. (2002),On yelucheyaet al. (2016), Wang et al. (2019) and Yuan et al. (2021).

It is noteworthy that from Table 4.9, the values of $K_1$ were higher than those of $K_2$ simply showing that the rate of glucose generation is high compared to its decomposition which is slow. This is in line with the findings of the work of Esther et al. (2012), Shi et al. (2017) and Santos et al. (2018) and Yuan et al. (2021).

The value of $\propto$ is in the range of 0.02-0.04 mg/mg with an average of 0.03 mg/mg indicating that 0.3% glucan was susceptible to hydrolysis which is smaller as compared to the works of Aguilar et al. (2002) and da Costa Lopes & Łukasik (2018). This was also affected by acid concentration as it increased with an increase in the concentration of the acid.

The glucose concentrations were again fitted into both the Saeman and Two-fraction models for the nitric acid hydrolysisas shown in Tables 4.20 and 4.21. Comparing the values of the statistical parameter (Adjusted $R^2$), and it was again found that the two-fraction model fits better. This result also agrees with those of Aguilar et al. (2002), Onyelucheya et al. (2016)and Yuan et al. (2021).

The kinetic parameters of decomposition reactions of glucose $K_2$ is in the same range of $K_1$. It can be supposed that this is due to high rate of degradation of glucose. This is in line with the findings in the work of Aguilar et al. (2002)and Negahdaret al. (2016).

The parameter $\propto$ was in the range of 0.03-0.06 mg/mg. it was slightly affected by increase in acid concentration, as also suggested by Onyelucheya et al. (2016) and Wang et al. (2019).

To substantiate the fact that the Two-fraction model is better compared to the Saeman's model, from Tables 4.10, 4.11, 4.12, 4.13, 4.14, 4.22, 4.23, 4.24, 4.25 and 4.26, comparing their third column (Saeman's model) with the fourth column (Two-fraction model) of the same Tables, the values from the fourth column arealmost always closer to the experimental values.

The maximum glucose production was predicted as 5wt% $H_3PO_4$ for 42mins, which gave 0.038mg/ml with 0.4% susceptibility to hydrolysis. Whereas the maximum glucose production was predicted as 2wt% $HNO_3$ for 77mins, which gave 0.054mg/ml with 0.6% susceptibility to hydrolysis.

Comparing these results with the maximum production obtained by Laboratory confirmation test; for glucose production at 5wt% $H_3PO_4$ for 42mins, gave 0.037mg/ml, where as using nitric acid as a catalyst, glucose production at 2wt% $HNO_3$ for 77mins, gave 0.046mg/ml of glucose.

And comparing these results with the maximum production obtained by Laboratory confirmation test and previous researchers; Antonio et al. (2004) in their "hydrolysis of sugarcane bagasse using nitric acid", the maximum conditions selected were 122$^o$C, 6wt% and 9.3mins which gave 2.87mg/ml of glucose. Yuan et al. (2021) confirmed these conditions with similar result in their recent research.

Sara et al. (2006) in their work, "Study of the hydrolysis of sugar cane bagasse using phosphoric acid", hadmaximum conditions selected at 122$^o$C, 4wt% and 300mins, which gave 3.0mg/ml of glucose, which has been corroborated by the findings of Shi et al. (2017).

Esther et al. (2012), in their study on "Acid hydrolysis of wheat straw" using sulphuric acid as a catalyst, the maximum conditions selected were 2wt% of $H_2SO_4$ at

$130^oC$ for 29mins, which gave glucose concentration of 3.5mg/ml with 11% susceptibility. And On yelucheya et al. (2016) in their acid hydrolysis of cassava peel using phosphoric acid, the maximum glucose concentration was obtained as 2.218mg/ml at 7.5wt%, 1min and $121^oC$.
From the results compared above, the glucose concentration is low, indicating a small degradation of the cellulosic fraction.

## V. CONCLUSSION

Kinetic study of the acid hydrolysis of corn cob to determine the yield of glucose has been established in this work. It has shown that corn cob is richer in hemicellulose content than cellulose, and this made it a weak source of glucose. Again, it has been shown that the rate of decomposition of the polymer ($K_1$) is greater than the rate of degradation of the monomer ($K_2$). Two-fraction model is found to be a better model for fitting of the hydrolysis data, as it gave better fits over the Seaman's model, and the parameter$\propto$ is less than or equal to 1 and is slightly affected by increase in acid concentration.
A maximum concentration of 0.038 mg/ml glucose was produced when 5wt% $H_3PO_4$ was used as catalyst for the hydrolysis, and a time interval of 42mins, with 0.4% susceptibility to hydrolysis, whereas for the nitric acid hydrolysis, 0.054mg/ml maximum glucose concentration was produced using 2wt% of the nitric acid, at a time interval of 77mins, with 0.6% susceptibility to hydrolysis. And comparing the results obtained using phosphoric acid and nitric acid, it has been established that the nitric acid is a more efficient catalyst for the hydrolysis.
Also, the results obtained from this research within the already established operational conditions shows that corn cob as a lignocellulosic material is suitable for the production of glucose.

## VI. REFERENCES

[1]. Alessandra V., Isabella D.B., Emanuele R. and Vincenza C. (2012). "Hydrolysis of Lignocellulosic Biomass Current Status of Processes and Technologies and Future Perspectives, Bioethanol, Prof. Marco Aurelio Pinheiro Lima (Ed.)", ISBN: 978-953-51-008-9.

[2]. Agarry S.E., Ajani A.O. and Agbede O.O. (2011). "A Comparative Kinetic Study of Acidic Hydrolysis of Wastes Cellulose from Agricultural Derived Biomass", Journal of Applied Science and Environmental Management, Vol. 15, pp. 531-537.

[3]. Aguilar R., Ramirez J.A., Garrote G., and Va´zquez M. (2002). 'Kinetic study of the hydrolysis of sugar cane bagasse'. Journal of Food Engineering. Vol.55, pp.309-318.

[4]. Arun B. and Bahl B.S. (2010), "A Textbook of Organic Chemistry", 19thRevised Edition, S. Chad and Company Ltd, pp. 638-641.

[5]. Andérez Fernández M., Rissanen J., Pérez Nebreda A., Xu C., Willför S., García Serna J. (2018). Hemicelluloses from Stone pine, Holm Oak, and Norway spruce with Subcritical Water Extraction − Comparative Study with Characterization and Kinetics. J. Supercrit. Fluids 133, 647–657. doi:10.1016/j.supflu.2017.07.001.

[6]. Antonio R.C., Jose A.R., Gril G. and Manuel V. (2004). "Hydrolysis of Sugarcane Bagasse using Nitric Acid: A Kinetic Assessment", Journal of Food Engineering, Vol. 61, pp. 142-152,

[7]. Bader S. and James D. (2013). "Results from the Xylitol for Adult Caries Trial (X-ACT)". The Journal of the American Dental Association. 144 (1). pp. 21–30.

[8]. Converti A., Parego P. and Dominguez J.M. (1999). "Xylitol Production from Hardwood Hemicellulose Hydrosylates" (PDF). Applied Biochemistry and Biotechnology. Vol. 82, pp. 141–151.

[9]. da Costa Lopes A.M. and Łukasik R.M. (2018). Separation and Recovery of a Hemicellulose-Derived Sugar Produced from the Hydrolysis of Biomass by an Acidic Ionic Liquid. ChemSusChem 11 (6), 1099-1107. doi:10.1002/cssc.201702231.

[10]. Delbecq F., Wang Y.,MuralidharaEl-Ouardi A. K., El-Ouardi K.,Marlair G. and Len C. (2018). Hydrolysis of Hemicellulose and Derivatives-A Review of Recent Advances in the Production of Furfural. Front. Chem. 6, 146. doi:10.3389/fchem.2018.00146.

[11]. Eken-Saraçoğlu N., Mutlu S.F., Dilmaç G. and Çavuşoğlu H. (1998). A comparative kinetic study of acidic hemicellulose hydrolysis in corn cob and sunflower seed hull. Bioresource Technolgy. Vol 65 (1-2), pp. 29-33.

[12]. Esther G.R., Oscar M.P., Lorenzo J.E., Jose A.R. and Manuel V. (2012). "Acid Hydrolysis of Wheat Straw: A kinetic Study", Biomass and Bioenergy, Vol. 36, pp. 346-35.

[13]. Guo Z., Ling Z., Wang C., Zhang X. and Xu F. (2018). Integration of facile deep eutectic solvents pretreatment for enhanced enzymatic hydrolysis and lignin valorization from industrial xylose residue. Bioresour Technol 265: pp. 334–339.

[14]. Herrera A., Te´llez-Luis S.J. and Va´zquez M. (2003). Production of xylose from sorghum straw using hydrochloric acid. J Cereal Sci;37(3), pp.267-74.

[15]. Islam S.M.R. and Mimi S. (2011). Kinetic Modeling of the Acid Hydrolysis of Wood Sawdust. International Journal of Chemical and Environmental Engineering, 2 (5) pp. 333-337.

[16]. Jeevan P., Nelson R. and Edith R. (2011). Optimization studies on acid hydrolysis of corn cob hemicellulosic hydrolysate for microbial production of xylitol. Journal of Microbiology and Biotechnology Research, Vol. 4, pp. 114-123.

[17]. Kalyani D.C., Fakin T., Horn S.J. and Tschentscher R. (2017). Valorisation of woody biomass by combining enzymatic saccharification and pyrolysis. Green Chem 19: pp. 3302–3312.

[18]. KapuN.S., Yuan Z., Chang X.F., Beatson R., Martinez D.M. and Trajano H.L. (2016). Insight into the Evolution of the Proton Concentration during Autohydrolysis and Dilute-Acid Hydrolysis of Hemicellulose. Biotechnol. Biofuels 9, 224. doi:10.1186/s13068-016-0619-6.

[19]. Lavarack B.P., Griffin G.J. and Rodman D. (2002). "The Acid Hydrolysis of Sugarcane Bagasse Hemicellulose to Produce Xylose, Arabinose and other Products", Biomass and Bioenergy, Vol. 23, pp. 367-380.

[20]. Liang C., Hu Y., Guo L., Wu L. and Zhang W. (2017). Kinetic study of acid hydrolysis of corncobs to levulinic acid. BioResources; 12(2), pp. 4049-4061.

[21]. Negahdar L., Delidovich I. and Palkovits R. (2016). Aqueous-phase Hydrolysis of Cellulose and Hemicelluloses over Molecular Acidic Catalysts: Insights into the Kinetics and Reaction Mechanism. Appl. Catal. B: Environ. 184, 285–298. doi:10.1016/j.apcatb.2015.11.039.

[22]. Neureiter M., Danner H., Thomasser C., Saidi B. and Braun R. (2002). Dilute acid hydrolysis of sugar cane bagasse at varying conditions. Appl. Biochem. Biotechnol. 98, pp. 49-58.

[23]. Nigam P. and Singh D. (1995). "Processes for Fermentative Production of Xylitol- a Sugar Substitute". Process Biochemistry. 30, pp. 117–124.

[24]. Nguyen Q.A., Tucker M.P., Keller F.A. and Eddy F.P. (2000). Two-stage dilute acid pretreatment of softwoods. Applied Biochemistry Biotechnology; 84-86, pp. 561-576.

[25]. Onyelucheya O.E., Nwabanne J.T, Onyelucheya C.M., Adeyemo O.E. (2016). Acid Hydrolysis of Cassava Peel. International Journal of Scientific & Technology Research, 5(1). pp. 184-187.

[26]. Rodrı´guez-Chong A., Ramı´rez J.A., Garrote G. and Va´zquez M. (2004). Hydrolysis of sugar cane bagasse using nitric acid: a kinetic assessment. Journal Food Engineering; 61(2), pp. 143-52.

[27]. Saeman J.F. (1945). Kinetics of wood saccharification. Hydrolysis of cellulose and decomposition of sugars in dilute acid at high temperature. Industrial and Engineering Chemistry, 37, pp. 43–52.

[28]. Sánchez O.J. and Cardona C.A. (2008). Trends in biotechnological production of fuel ethanol from different feedstocks", Bioresource Technololgy 99, pp. 5270-5295.

[29]. Santos V. T. d. O., Siqueira G., Milagres A. M. F. and Ferraz A. (2018). Role of Hemicellulose Removal during Dilute Acid Pretreatment on the Cellulose Accessibility and Enzymatic Hydrolysis of Compositionally Diverse Sugarcane Hybrids. Ind. Crops Prod. 111, 722–730. doi:10.1016/j.indcrop.2017.11.053.

[30]. Sara Ga´mez, Juan Jose Gonza´lez-Cabriales, Gil Garrote B. and Manuel Va´zquez. (2006). Study of the hydrolysis of sugarcane bagasse using phosphoric acid. Journal of Food Engineering 74, pp. 78–88.

[31]. Shi S., Guan W., Kang L. and Lee, Y.Y. (2017). Reaction Kinetic Model of Dilute Acid-Catalyzed Hemicellulose Hydrolysis of Corn Stover under High-Solid Conditions. Ind. Eng. Chem. Res. 56 (39), 10990–10997. doi:10.1021/acs.iecr.7b01768.

[32]. Va´zquez M., Oliva M., Te´llez-Luis S.J., Ramı´rez J.A. (2007). Hydrolysis of sorghum straw using phosphoric acid: evaluation of furfural production. Bioresource Technology; 98:305360.

[33]. Wan L., Gao Z., Wu B., Cao F., Jiang M., Wei P. (2021). Hydrolysis of Corncob Hemicellulose by Solid Acid Sulfated Zirconia and its Evaluation in Xylitol Production. Appl. Biochem. Biotechnol. 193 (1), pp. 205–217.

[34]. Wang C., Yang G., Zhang X., Shao L., Mao J., Liu S. and Xu F. (2019). A kinetic study on the hydrolysis of corncob residues to levulinic acid in the FeCl3-NaCl system. Springer-Cellulose 26:8313-8323. https://doi.org/10.1007/s10570-019-02711-7.

[35]. Xu F., Shi Y.C., Wu X.R., Theerarattananoon K., Staggenborg S. and Wang D.H. (2011). Sulphuric acid pretreatment and enzymatic hydrolysis of photoperiod sensitive sorghum for ethanol production. Bioprocess Biosystems Engineering; 34(4):48592.

[36]. Yuan Q., Liu S., Ma M., Ji X., Choi S. and Si C. (2021). The kinetics studies on hydrolysis of hemicellulose. Frontiers in Chemistry; 9:781291. doi:10.3389/fchem.2021.781291.

[37]. Zhu S., Wu Y., Yu Z., Zhang X., Wang C. and Yu F. (2006). Production of ethanol from microwave-assisted alkali pretreated wheatstraw. Process Biochemistry; 41(4):869e73.